ELSEVIER

Polymer 40 (1999) 6545–6556

polymer

Conformational mobility in a polymer with mesogenic side groups Dielectric and DSC studies

J.F. Mano[a], N.M. Alves[a], J.M. Meseguer Dueñas[b,*], J.L. Gómez Ribelles[c]

[a]*Dept. Engenharia de Polímeros. Universidade do Minho. Campus de Azurém. 4800 Guimarães. Portugal*
[b]*Dept. Física Aplicada. Universidad Politécnica de Valencia. Ap. 22012, 46071 Valencia, Spain*
[c]*Dept. de Termodinámica Aplicada Universidad Politécnica de Valencia. Ap. 22012, 46071 Valencia, Spain*

Received 14 July 1998; received in revised form 30 November 1998; accepted 1 December 1998

Abstract

The relaxation times of the conformational rearrangements of the main-chain segments of a liquid crystalline side-chain polymer was determined from differential scanning calorimetry experiments in the temperature interval around and below its glass transition. Phenomenological models with fitting parameters were used to evaluate the temperature dependence of the relaxation times and the form parameter of the relaxation times distribution. These parameters were compared with its counterparts in the dielectric α relaxation process which appear in the temperature interval immediately above the calorimetric glass transition. For the temperature interval below the calorimetric glass transition the differential scanning calorimetry (DSC) results were compared with the dielectric results obtained by the thermally stimulated depolarisation technique.

Keywords: Differential scanning calorimetry; Dielectric spectroscopy; TSDC

1. Introduction

Thermotropic liquid crystalline polymers (LCPs) are hybrid materials, which combine the mechanical, and the rheological properties of polymeric substances with the anisotropic physical properties of low molecular weight liquid crystals [1–3]. Besides the academic interest, this combination of features confers upon these materials a versatility, which can be used in different applications, namely in optical information storage, non-linear optics and chromatography [3,4].

A class of these polymers, having been synthesised since the late 1970's [5–7], has side-chain mesogenic groups attached laterally to the main chain by means of a flexible link, usually an alkyl chain. The alkyl spacer $-(CH_2)_x-$, with length x is introduced to decouple, to some extent, the motion of the mesogen from that of the polymeric backbone [3].

The molecular dynamics behaviour of polymers with mesogenic side-group, or side-chain LCPs were the subject of intense research and, because of the polar nature which usually characterise the main-chain and the mesogenic group, dielectric relaxation spectroscopy (DRS), has proven to be a very suitable tool to study the different molecular motions in these compounds. The pioneering work in this field was carried out by Kresse and coworkers [8,9]. Since then much work from different groups has been published [10–33].

At low temperatures, below the glass transition temperature, T_g, side-chain LCPs are in the glassy state, like most of the conventional polymers, and exhibit locally involved relaxation processes, often labelled as β, γ,… with decreasing temperature. These relaxations were assigned to localised motions within the side-groups [11,14,15]. Above T_g these materials have liquid crystalline character up to the clearing temperature and two main relaxation mechanisms could be identified, named δ and α, in the order of increasing frequency.

It was suggested that these two major relaxations could be predicted by the four-mode theory [22,34], based in the rotational dynamic theory proposed by other authors [35,36]. According to this, the α relaxation should be related to the motions of the longitudinal component of the dipole moment of the mesogenic head group, $\mu_{\parallel}$, and the α relaxation should be mainly assigned to the motions of the corresponding transverse component of the dipole moment, $\mu_{\perp}$, rotating about the mesogen's long axis. Several authors followed these assumptions to interpret the origin of both δ and α processes at the molecular level [20–31]. Moreover, some experimental evidences, namely the dielectric

* Corresponding author.

0032-3861/99/$ - see front matter
PII: S0032-3861(98)00850-7

results obtained after a previous macroscopic alignment of the mesogenic groups in sample [19–31], supported these attributions. In fact, it was observed that, when the side groups were aligned along the direction of the electric field (homeotropic alignment), the strength of the δ relaxation was enhanced whereas the strength of the α relaxation was reduced, relatively to the unaligned state. However, the planar or homogeneous alignment (alignment of the mesogen's groups perpendicularly with respect to the electric field) showed the opposite effect [22,25,26,28–31].

However, the assignment of the α process observed in side-chain LCPs by dielectric spectroscopy has been controversial. In fact, another group of investigators interpreted this relaxation as corresponding to the so-called α relaxation observed in amorphous and semicrystalline conventional polymers, associated to the dynamic glass transition of the system [8–16]. In fact, some features of the LCPs' α process, namely the temperature location relatively to the calorimetric glass transition temperature, the well described temperature dependence of the relaxation time with the Vogel–Fulcher–Tammann–Hesse (VFTH) equation, and the corresponding activation energy range, are typical of the α relaxation of conventional polymers.

The dielectric permittivity, ε^*, of this process is related to a relaxation function, $\phi(t)$,by a pure imaginary Laplace transformation

$$\frac{\varepsilon^*(\omega)-\varepsilon_\infty}{\varepsilon_0-\varepsilon_\infty}\int_0^\infty -\dot{\phi}\ (t)\mathrm{e}^{-i\omega t}\mathrm{d}t. \tag{1}$$

It was shown that the α process as seen by dielectric relaxation in conventional polymers could be rationalized in terms of the total relaxation of the dipole moments, μ_j, of chain segments. The relaxation function is approximately the same as the dipole moment time correlation function which can be given in terms of the time variation of μ_j [37].

$$\phi(t)=\frac{\sum_i^n\sum_j^n\langle\mu_i(0)\cdot\mu_j(t)\rangle}{\sum_i^n\sum_j^n\langle\mu_i(0)\cdot\mu_j(0)\rangle}.$$

Therefore, the time evolution of this relaxation function is highly correlated with the spatial variation of the dipole moments μ_j, which occurs by means of rotations in the single covalent bonds along the polymeric chain. This means that this relaxation process is intimately related with the conformational motions of the main chain segments.

The relaxation times of the conformational rearrangements can be also obtained by differential scanning calorimetry (DSC) through the modelling of the structural relaxation process. Structural relaxation is the term that designates the process of approach to an equilibrium state undergone by a glass held at constant environmental conditions after its formation history [38–41]. The glass transition itself is the result of the exponential dependence of the structural relaxation times on temperature. Several phenomenological models were developed on the introduction of the reduced time [41] to linearize the equations of the relaxation process [43–46], thus applying a superposition principle to deduce an equation for the response to a complex thermal history.

The evolution of the enthalpy in response to a thermal history that consists of a series of temperature jumps from T_{i-1} to T_i at time instants t_i, followed by isothermal stages is given by:

$$H(t)=H^{\mathrm{eq}}(T(t))-\sum_{i=1}^{n}\left(\int_{T_{i-1}}^{T_i}\Delta c_{\mathrm{p}}(T)\mathrm{d}t\right)\phi(\xi-\xi_{i-1}), \tag{2}$$

where $\Delta c_{\mathrm{p}}(T)=c_{\mathrm{pl}}(T)-c_{\mathrm{pg}}(T)$ is the configurational heat capacity, the difference between the heat capacity in the equilibrium liquid state and that of the glassy state and ξ is the reduced time.

$$\xi=\int_0^t\frac{\mathrm{d}t'}{\tau(t')}. \tag{3}$$

The relaxation function ϕ is assumed of the Kohlrausch–Williams–Watts [47] type in the most applied models:

$$\phi(\xi)=\exp(-\xi^{\beta}). \tag{4}$$

The relaxation time $\tau(t)$ in Eq. (3) is a function of both temperature and the separation from equilibrium measured by the fictive temperature, which links any out of equilibrium state at temperature T with an equilibrium one [42,43]. The fictive temperature can be calculated from enthalpy data through

$$\int_{T_{\mathrm{f}}}^{T^*}(c_{\mathrm{pl}}(T)-c_{\mathrm{pg}}(T))\mathrm{d}T=\int_{T}^{T^*}(c_{\mathrm{p}}(T)-c_{\mathrm{pg}}(T))\mathrm{d}T, \tag{5}$$

where T^* is a temperature above the glass transition.

In the model proposed by Narayanaswamy [42] and then by Moynihan and his group [43] (hereafter the NM model) the double dependence of the relaxation time on temperature and structure is expressed by

$$\tau(T,T_{\mathrm{f}})=A\exp\left(\frac{\Delta h^*}{R}\left(\frac{x}{T}+\frac{1-x}{T_{\mathrm{f}}}\right)\right), \tag{6}$$

where x is a parameter between 0 and 1. Eq. (6) reduce to an Ahrrenius dependence for the relaxation time in equilibrium ($T_{\mathrm{f}}=T$) with Δh^* an apparent activation energy.

Alternatively, in the model proposed by Scherer [44] and Hodge [45] (called hereafter SH model) an expression deduced from the Adam–Gibbs [48] theory is applied

$$\tau(T,S_{\mathrm{c}})=A\exp\left(\frac{B}{TS_{\mathrm{c}}(\xi,T)}\right), \tag{7}$$

where S_{c} is the configurational entropy. Assuming $\Delta c_{\mathrm{p}}(T)=T_{\mathrm{g}}\,\Delta c_{\mathrm{p}}(T_{\mathrm{g}})/T$ one arrives to [45]

$$\tau(T,T_{\mathrm{f}})=A\exp\left(\frac{D}{RT(1-T_2/T_{\mathrm{f}})}\right), \tag{8}$$

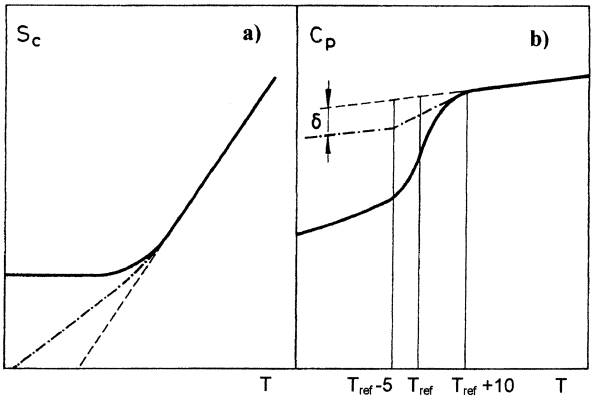

Fig. 1. (a) Sketch of the configurational entropy corresponding to the liquid state (dashed line), to an experimental cooling scan at a finite cooling rate (solid line), and to the hypothetical line of the limit states of the structural relaxation process (dashed–dotted line). (b) $c_p(T)$ lines corresponding to the three cases described in a): the dashed line corresponds to the liquid state $c_{pl}(T)$ the solid line corresponds to an experimental cooling scan, and the dashed–dotted line corresponds to the specific heat capacity in the limit states of the structural relaxation process: $c_p^{lim}(T)$.

where T_2 is the Gibbs–DiMarzio [49] transition temperature. Eq. (8) reduces to a Vogel equation in equilibrium.

In both NM and SH models four parameters describe the structural relaxation process (Δh^*, x, A, and β in NM model and D, T_2, A, and β in SH model). These parameters are assumed to be material parameters, and so independent from the thermal history. Nevertheless it was shown that it is difficult to reproduce with a single set of model parameters the $c_p(T)$ curves measured in DSC heating scans after different thermal histories [50–53].

One of the main assumptions in the aforementioned models is that an amorphous material kept in isothermal conditions in any of equilibrium states would reach, at infinite time, an equilibrium state determined by the extrapolation to temperatures below T_g of the enthalpy equilibrium line determined at temperatures above the glass transition. This comes from the identification of the limit of the fictive temperature at infinite time with T. Recently a model has been proposed in which the limit at infinite time of the structural relaxation process is considered to be a metaestable state with higher configurational entropy and enthalpy than the equilibrium state obtained by extrapolation. This situation would come from the collapse of the configurational rearrangements when the number of configurations available for the polymer segments would attain a certain limit. When this limit is reached, the system is in a metaestable state and no further decrease in the configurational entropy is possible. Thus the equilibrium states would not be attainable with the kind of processes described in this work.

To introduce this hypothesis the model equations were expressed in terms of the configurational entropy

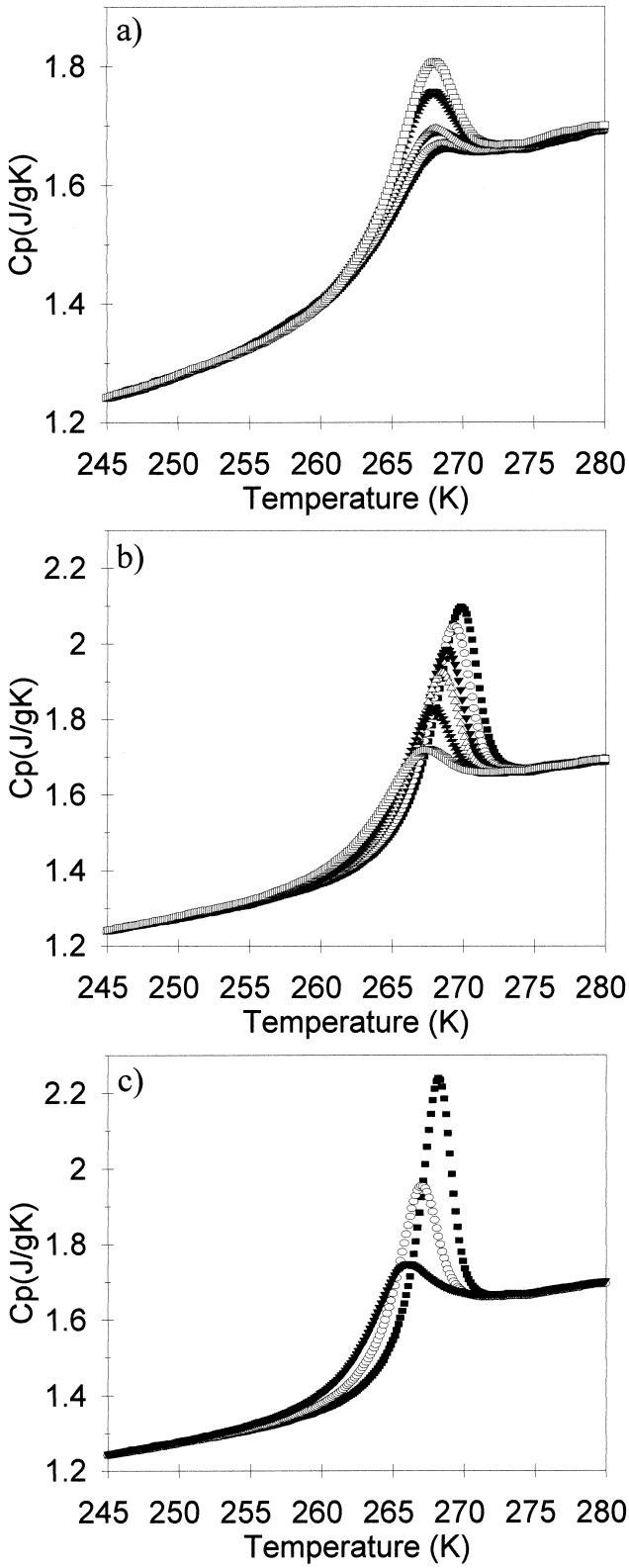

Fig. 2. Experimental $c_p(T)$ curves measured in heating scans after different thermal histories (a) Cooling at 1 (□), 2 (⧗), 5 (△), 10 (▼), 20 (○) and 40°C/min, (b) $T_a = -15$°C, t_a 1176 (■), 305 (○), 120 (▼), 80 (△), 20 (⧗) and 5 min (□) (c) $T_a = -23$°C, t_a 860 (■), 263 (○) and 76 min (▼).

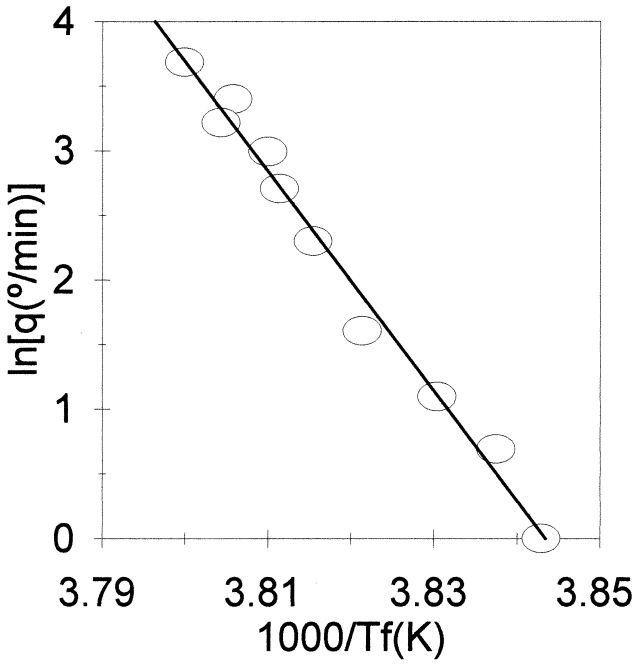

Fig. 3. Fictive temperature in the glassy state after cooling at different cooling rates q_c from the liquid state.

[54,55].

$$S_c(t) = S_c^{lim}(T(t)) - \sum_{i=1}^{n}\left(\int_{T_{i-1}}^{T_i} \frac{\Delta c_p^{lim}(T)}{T} dT\right)\phi(\xi - \xi_{i-1}), \quad (9)$$

where $S_c^{lim}(T)$ is the configurational entropy in the metaestable limit states. To describe this function it is necessary to introduce new model parameters what, in principle, is not desirable. To reduce the number of new parameters to a minimum $S_c^{lim}(T)$ was defined as shown in Fig. 1(a) (dashed–dotted line). The slope of the $S_c^{lim}(T)$ curve is smaller than the one of the configurational entropy in equilibrium $S_c^{eq}(T)$ at temperatures below the glass transition. The change of slope approaching the equilibrium values is gradual covering a temperature interval of 15 K. The change of slope shown in the sketch of Fig. 1(a), determined by the reference temperature T_{ref}, should be quite coincident with the glass transition temperature interval. We will take in the calculations a value for T_{ref} equal to the glass transition temperature determined from the intersection of the enthalpy lines corresponding to the liquid and the glassy states. In this way a single additional parameter δ defined in Fig. 1, is introduced in the model.

In Eq. (9) the reduced time is given by Eq. (3), the relaxation function is the KWW Eq. (4) and the relaxation time is given by the Adam–Gibbs expression (7), which needs no further manipulation to be introduced in (9). $\Delta c_p^{lim}(T)$ is defined through:

$$S_c^{lim}(T_i) - S_c^{lim}(T_{i-1}) = \int_{T_{i-1}}^{T_i} \frac{\Delta c_p^{lim}(T)}{T} dT \quad (10)$$

thus, if T^* is a temperature above the glass transition region, for any temperature T, in the glass transition temperature interval or below

$$S_c^{lim}(T) = S_c^{eq}(T^*) = \int_{T^*}^{T} \frac{\Delta c_p^{lim}(T)}{T} dT, \quad (11)$$

$$S_c^{eq}(T) = \int_{T_2}^{T} \frac{\Delta c_p(T)}{T} dT. \quad (12)$$

It has been shown [54–59] that the agreement between the model simulation and the experiments is highly improved when the values of $S_c^{lim}(T)$ are significantly higher than that of $S_c^{eq}(T)$.

It was also shown that structural relaxation results, obtained by differential scanning calorimetry (DSC) measurements, could be well correlated with the dynamic glass transition of polymeric systems as observed by dielectric relaxation spectroscopy [54,57,59]. In this work the study of the structural relaxation of a side-chain LCP in the glass transition region is reported. The results are compared with previously published dielectric spectroscopy results on the same compound [33] in order to elucidate the nature of the α relaxation observed in this kind of materials.

2. Experimental

The liquid crystalline polymer studied in this work is from Merck (catalogue no. LCP1) and has the following structure

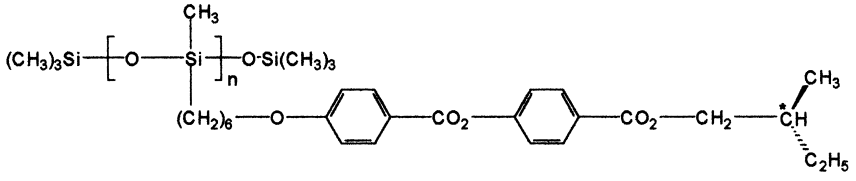

with $n \sim 40$ According to the manufacturer, it has a glass transition temperature near −7°C and a smectic C/isotropic transition at 76.8°C.

The differential scanning calorimetry, DSC, experiments were carried out in a Perkin–Elmer DSC7 differential scanning calorimeter with controlled cooling accessory. The temperature of the equipment was calibrated with indium

and lead standards and for the heat flow calibration only the same indium sample was used. Calibration of the absolute heat capacity was performed using sapphire. All calibrations were carried out during heating, at 10°C/min.

The weights of sample and reference pans were matched to within 0.01 mg and a LCP1 sample weighing 10.293 mg was used. All the experiments on LCP1 started at 50°C with the sample in equilibrium. Thermal histories included cooling at different rates as well as isothermal annealing stages at different temperatures, T_a, over different time intervals, t_a. The measuring scan was carried out during subsequent heating scans at a constant rate, 10°C/min, from −50°C to 50°C.

3. Results

The $c_p(T)$ curves measured in heating scans after different thermal histories are shown in Fig. 2. When the thermal history of the glassy sample consists in a cooling from a temperature above T_g, the effect of the cooling rate is analogous to that of any other amorphous material, i.e., when the cooling rate decreases the height of the peak that appears in $c_p(T)$ in the high temperature side of the glass transition increases (Fig. 2(a) shows only some of the experimental curves measured after this type of thermal history). The shape of this peak is a measure of the glass transition temperature, or the fictive temperature attained in the glassy state after the cooling down process, $T_{f'}$, as it can be calculated using Eq. (5) for the lowest temperature attained in the cooling process. This temperature is the glass transition temperature determined by the intersection point of the enthalpy lines in the equilibrium liquid and the glassy states.

The value of the fictive temperature in the glassy state $T_{f'}$ is represented in Fig. 3 as a function of the cooling rate q_c in a $\ln q_c$ vs. $1/T_{f'}$ plot. The well known relationship between the slope in this diagram and the temperature dependence of the relaxation times of the structural relaxation around the glass transition [60] allows to determine an apparent activation energy Δh^* of the conformational rearrangements in the narrow temperature interval around the glass transition

$$\frac{\mathrm{d}\ln\tau^{eq}}{\mathrm{d}1/T} = -\frac{\mathrm{d}\ln q_c}{\mathrm{d}1/T_{f'}} = \frac{\Delta h^*}{R}, \tag{13}$$

where τ^{eq} indicates the relaxation time in equilibrium, and R is the gas constant. With this procedure a value of $\Delta h^*/R =$ 85 kK was found for this glass transition.

When the thermal history previous to the measuring scan contains an annealing period, the $c_p(T)$ experimental curve shows the characteristic peak that shifts to higher temperatures and increase in intensity as the annealing time increases. The Fig. 2(b) and (c) show this behaviour at two annealing temperatures, −15 and −23°C which are 5.5° and 13.5° below the glass transition temperature determined from the $c_p(T)$ curve measured after cooling at 40°C/min which will be called hereafter the T_g of this sample.

4. Discussion

The temperatures at which appears the α dielectric relaxation process justify the first hypothesis that its origin is closely related to the glass transition process observed in DSC. The phenomenology of the latter should be related to the vitrification process produced by the lack of most of the conformational mobility of the main chains of the polymer as the temperature decreases in the range of the glass transition as has been extensively discussed in amorphous polymers. Nevertheless as discussed in Section 1 other ascriptions for the dielectric relaxation process are possible: more local motions in the mesogenic groups which in principle, as secondary relaxations, would not be detected in DSC experiments. If this interpretation is accepted the appearance of the α relaxation at temperatures immediately above the glass transition would have to be studied from a different point of view.

To prove the close relation between the α relaxation process and the DSC glass transition, and so with the loose of the conformational mobility with decreasing temperature along the relaxation interval, it is necessary a more detailed comparison of the characteristics of both processes. These means to be able to compare the temperature dependence of the relaxation times of the dielectric relaxation and the structural relaxation and the width of the relaxation times distribution as well. The obvious difficulty is that the DSC thermograms do not provide a direct measure of these parameters. The modelling of the structural relaxation process is a useful tool to go from experiments to the phenomenology of the structural relaxation phenomenon in terms of the characteristics of the relaxation times.

4.1. Modelling of the DSC results

To determine the relaxation times of the conformational rearrangements form the DSC experimental results a series of six $c_p(T)$ curves were reproduced with the model equations with the same model parameters that are considered material parameters independent from the thermal history. To do this the heating and cooling ramps were simulated with a series of 1° temperature steps followed by isothermal stages to give the same average temperature change than in the experiments. It has been shown [61,62] that the temperature gradients inside the DSC sample during a heating scan at 10°C/min are between 0.5° and 1° depending on the thickness of the sample and the thermal contact between the sample and the sample pan and between the sample pan and the instrument cup. In some way the experimental result averages the properties of the sample in 0.5°–1° temperature interval. The evaluation of the model equations in 1° steps simulates this fact. Anyway all the experimental scans were measured at the same heating rate and thus it is expected that the thermal gradients be the same in all of them, as the fitting routine reproduces simultaneously all the

Table 1
Set of model parameters found by the search routine for LCP1 with different values of parameter B

B(J/g)	δ	β	T_2 (°C)	$T_g - T_2$(deg)	ln (A/s)
500	0.07 ± 0.02	0.35 ± 0.01	−43.5 ± 0.2	34	−38.7 ± 0.3
1000	0.06 ± 0.02	0.38 ± 0.01	−57.4 ± 0.2	48	−51.6 ± 0.3
1500	0.06 ± 0.02	0.41 ± 0.01	−67.8 ± 0.2	58	−60.2 ± 0.3

experimental scans, the effect of thermal gradients should be a small error in the values of the model parameters determined. In Ref. [62] the thermal gradients were introduced in the NM model equations and no significant difference in the main features of the model fit was found. The expression accepted for the configurational heat capacity was taken as the average of those found for the complete set of experimental results: $\Delta c_p(T) = 1.011–0.0028T$ J/(gK). The model parameters were determined by the Nedler and Mead [63] least squares routine, looking for a minimum in the total fitting error in the six $c_p(T)$ curves.

Owing to the correlation existing between B, T_2 and ln A, reported in different polymers, the value of B was fixed and the set of four parameters δ, β, T_2 and ln A were determined with the least squares routine. The procedure was repeated with different values of B. The Table 1 include the results obtained with B ranging between 500 and 1500 J/g. The three sets of parameters yield $c_p(T)$ curves nearly superposed as, as we will discuss later, they yield relaxation times practically identical in the range between 10^{-3} to 10^3 s, which is significant for the experiments. The model simulated curves for $B = 1000$ J/g are shown in Fig. 4 together with the experimental ones. The agreement in the main features is good, nevertheless some details are not reproduced such as the small peak in the $c_p(T)$ measured after cooling at the highest cooling rate. This fact cannot be attributed to the characteristics of this particular thermal history but to the fitting procedure in which the error function to minimise is a sum of the error in the different curves in which those with higher values of c_p, i.e., those showing the highest peaks have stronger influence. Anyway the overall fit can be considered acceptable and the model parameters found a good description of the behaviour of this LCP with respect to the glass transition and structural relaxation phenomenon.

The complete fitting procedure was conducted with different sets of experimental results in order to check the consistency of the method. This allows to estimate the uncertainty in the different model parameters shown in Table 1.

It is not crucial for our methodology to decide which is the best set of parameters between those shown in Table 1, i.e. to decide which is the correct value of B. This point has been extensively discussed in the case of poly(vinyl acetate) in terms of the length of cooperativity at the glass transition temperature [59]. For $B = 500$ J/g the value of the preexponential factor $A = 1.5\ 10^{-17}s$ is the most realistic, and it grows quickly as B increases. On the contrary the difference $T_g - T_2$ is lower than expected from viscoelastic data while keeps around 50° for $B = 1000$ J/g.

In Fig. 5 we represent the equilibrium relaxation times calculated from

$$\tau^{eq}(T) = A \exp\left(\frac{B}{TS_c^{eq}(T)}\right) \tag{14}$$

for $B = 500$ and $B = 1000$ J/g showing that in practice both sets of parameters reproduce the same material function: the temperature dependence of the relaxation times in equilibrium, which is uniquely determined from the DSC experiments. Probably higher values of B are not realistic in this polymer. The slope of the ln τ^{eq} vs. $1/T$ at T_g can be calculated from Eq. (14) once the model parameters are known. A value ranging between 73.1 and 81.5 kK is found for the temperature interval between 260.3 and 263.5 K (the glass transition temperatures measured after cooling at 1°C and 40°C/min, respectively) with the set of parameters corresponding to $B = 1000$ J/g not far from the value of $\Delta h^*/R$ calculated from the dependence of the glass transition temperature on the cooling rate.

The relaxation times shown in Fig. 5 are, at low temperatures, very far from the relaxation times in the out of equilibrium states of the material during the experimental scan. The model is able to calculate the values of the relaxation time in the heating ramp in 1° steps. This function calculated for the DSC scan that follows the cooling down at 40°C/min is represented in Fig. 6. At low temperature, at the beginning of the heating ramp the material behaves as a glass, this means that only the instantaneous or zero time response to the temperature changes is measurable because the relaxation times are much higher than the experimental times. In the model equations this means that the configurational entropy becomes temperature independent in this temperature interval, and thus the relaxation time in the glassy state depends on the temperature according to an Ahrrenius equation:

$$\tau^g = (T) = A \exp\left(\frac{B}{TS_c^g}\right), \tag{15}$$

where S_c^g depends on the thermal history in the formation of glass but not on the instantaneous temperature. The slope of the relaxation times in the glass in an Ahrrenius plot can be expressed in form analogous to that of Eq. (6)

$$\frac{\mathrm{d}\ \ln\tau^g}{\mathrm{d}1/T} = \frac{x\Delta h^*}{R}, \tag{16}$$

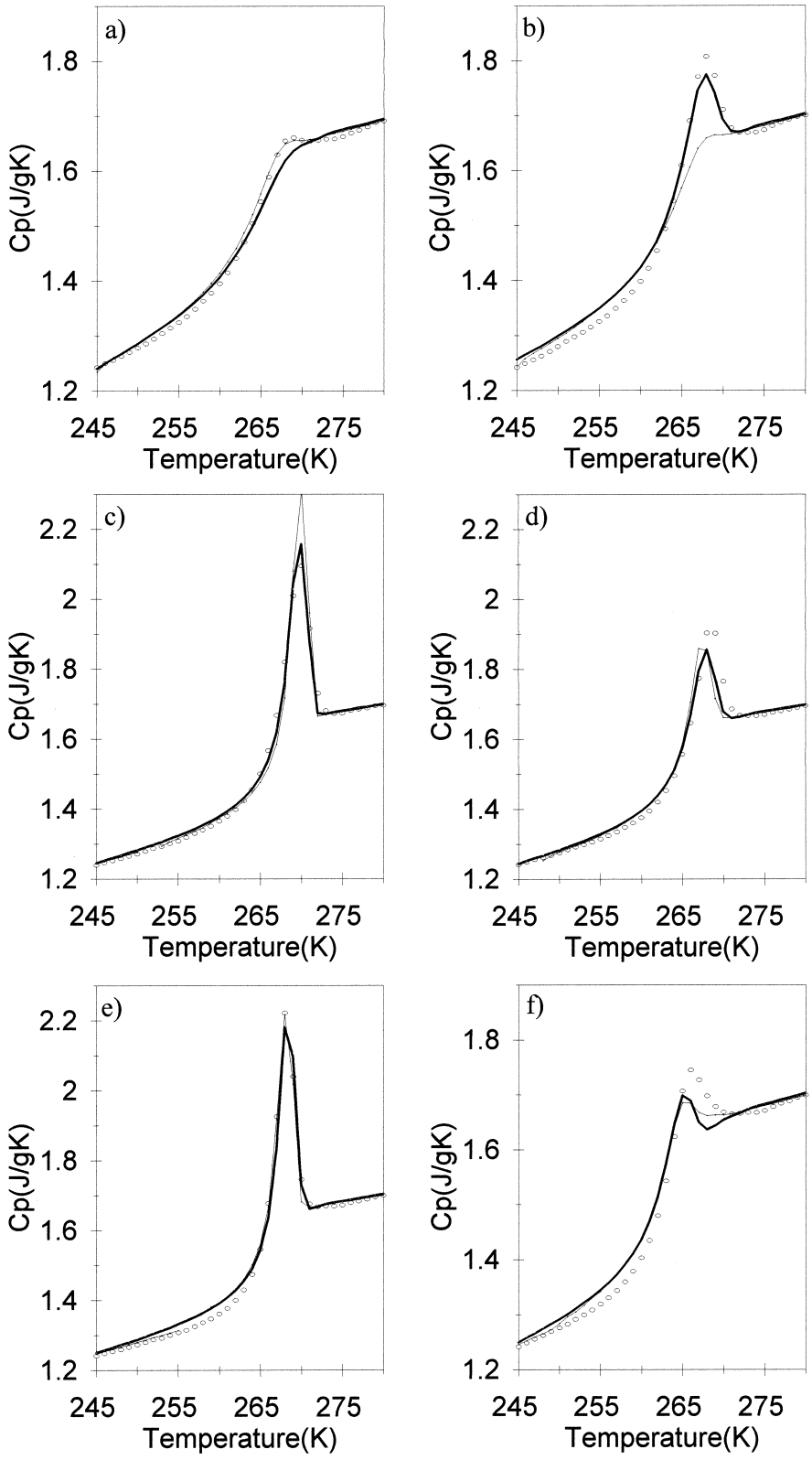

Fig. 4. Temperature dependence of the heat capacity of LCP1 measured after different thermal treatments (open circles): (a) Cooling at 40°C/min, (b) Cooling at 1°C/min, (c) $T_a = -15$°C, $t_a = 1176$ min, (d) $T_a = -15$°C, $t_a = 60$ min, (e) $T_a = -23$°C, $t_a = 860$ min, (f) $T_a = -23$, $t_a = 76$ min. The full line represents the model calculated curves with $B = 1000$ J/g and the rest of parameters as given in Table 1.

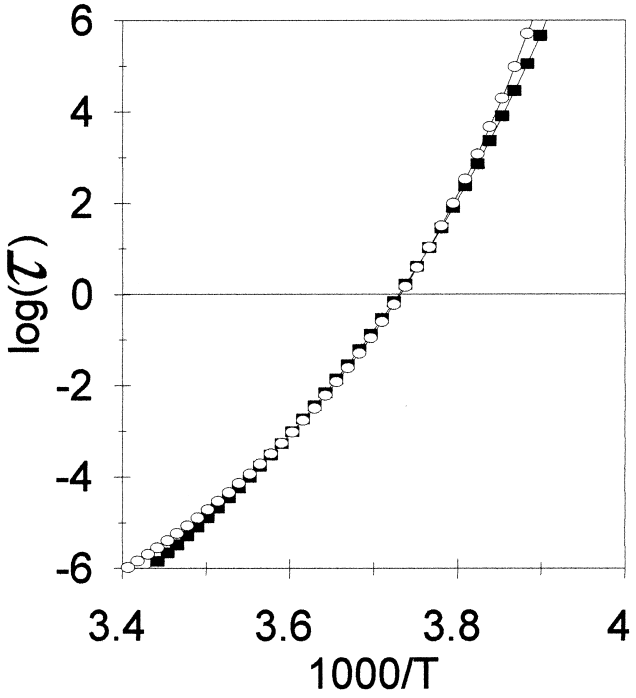

Fig. 5. Temperature dependence of the equilibrium relaxation times, $\tau^{eq}(T)$, calculated with $B = 500$ J/g (○) and $B = 1000$ J/g (■) (the rest of parameters according to Table 1).

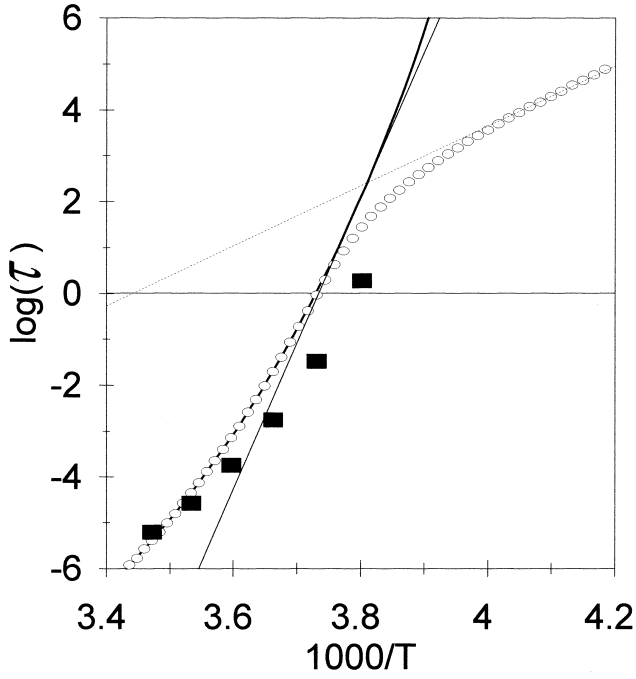

Fig. 6. Relaxation time of the structural relaxation process calculated by the model for a heating scan at 10°C/min after cooling the sample at 40°C/min from the equilibrium liquid state. The straight lines represent the temperature dependence in the glassy state and in the liquid state around the glass transition temperature, both assuming Ahrrenius behaviour. The squares represent the dielectric relaxation times.

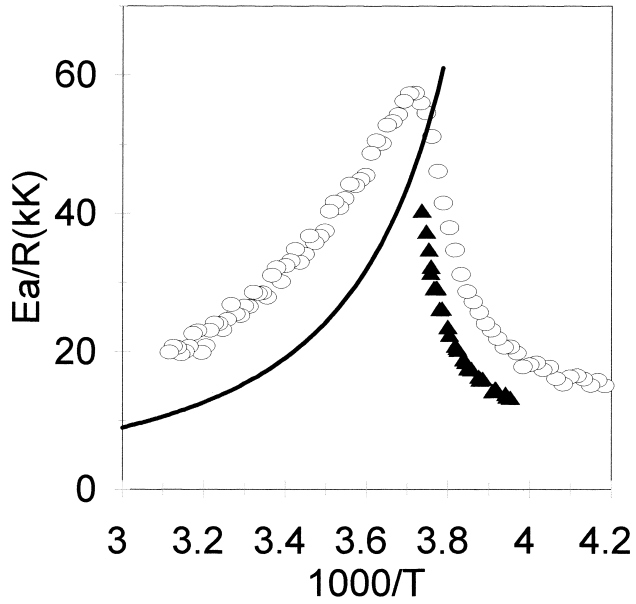

Fig. 7. Slope of the log τ vs. 1/T plot, obtained form DSC (○), DRS (full line) and thermal sampling experiments (▲). See text.

with

$$\frac{x\Delta h^*}{R} = \frac{B}{S_c^g}. \tag{17}$$

The relaxation times obtained from the modelled reference scan we can obtain $x\Delta h^*/R = 15.1$ kK as the apparent activation energy in the glassy state which yields $x = 0.21$. For different thermal treatments one obtain different values of S_c^g and, thus, different values of x. This means that in the framework of this model x is not a material parameter. In other words the temperature dependence of the relaxation times in the glassy state depends on the thermal history in the formation of glass.

This can be further clarified by representing an apparent activation energy, defined by

$$\frac{\mathrm{d}\ln\tau}{\mathrm{d}1/T} = \frac{Ea}{R} \tag{18}$$

against the reciprocal of temperature (Fig. 7). The open symbols represent the values of Ea/R calculated from the model simulated curve of relaxation times represented in Fig. 6 for the heating scan which follows a cooling from equilibrium at 40°C/min. At high temperatures, in the liquid state Ea increases as the temperature decreases according to a VFTH-like equation. At a temperature above but close to the glass transition temperature the relaxation times start deviating from the equilibrium line and thus the value of the slope Ea/R decreases, approaching at low temperatures the value corresponding to the glassy state. The maximum in the representation of Fig. 7 appears, thus, at the temperature at which the relaxation times separates from their equilibrium values.

The set of results obtained from this model should be very

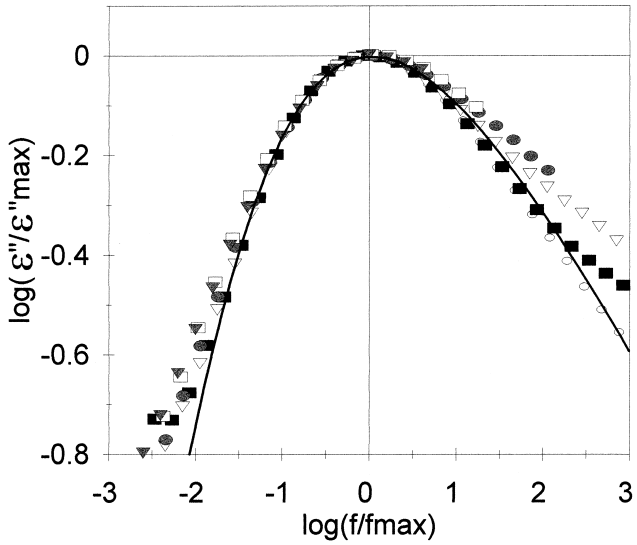

Fig. 8. Master curve for the imaginary part of the complex dielectric permittivity obtained from five isotherms (○) − 10°C, (■) − 5°C, (▽), 0°C, (●) 5°C, (□) 10°C, (▼) 15°C. The full line represent the KWW equation with $\beta = 0.35$.

close to those obtained using SH model as the value of the parameter δ found by the fitting routine is small. Nevertheless it is interesting to compare them with the results obtained using the NM model. The procedure followed was analogous to the one described earlier. The set of six experimental thermograms was fitted simultaneously to the NM model considering the model parameters Δh^*, x, A and β as material parameters. It is important to note that it is not equivalent to assume that the parameters depend on the thermal history to accept that they can take different values for the modelling of the different experimental $c_p(T)$ curves. In particular, the parameter x was considered as a constant in the deduction of the whole set of model equations in the case of the NM model, and to change this assumption would modify them.

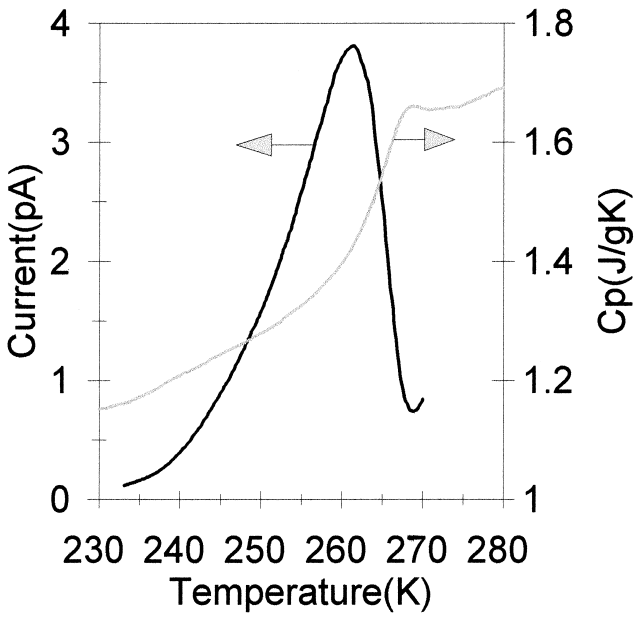

Fig. 9. Comparison between global TSDC peak measured in the temperature range of the α relaxation of LCP1 and the $c_p(T)$ curve measured in a heating scan after a cooling at 40°C/min. The TSDC experimental conditions were $T_p = 30$°C, $t_p = 10$ min $T_d = -50$°C, Polarizing field $E = 900$ V/mm, Heating rate 4°C/min.

In the fitting procedure the fictive temperature was calculated from the $c_p(T)$ curves using the Eq. (4). The value of $\Delta h^*/R = 85$ kK obtained from the results shown in Fig. 3 was fixed in the fitting routine which yield to the set of parameters $x = 0.19$, $\beta = 0.35$, $\ln A = -316$. It is important the close agreement in the value of the parameters x and β with those found with the SC model. The set of model simulated curves are represented in Fig. 4. The agreement is clearly poorer than in the SC model as the peak in the thermogram measured after cooling at 1°C/min is not shown in the model calculated curve. Of course this individual experimental result can be reproduced with the model but the values of the parameters needed to do that are quite different than those found in the simultaneous least squares routine: $x = 0.27$, $\beta = 0.50$, $\ln A = -316.7$.

4.2. Dielectric relaxation times

The dielectric results measured in the frequency domain in the region of the α relaxation were reported in the Ref. [33]. This relaxation process appears in the temperature interval immediately above the glass transition determined by DSC as occurs in the main dielectric relaxation process of the amorphous materials. From these data it is possible to built a master curve (Fig. 8) of the imaginary part of the dielectric permittivity ϵ'' as a function of the logarithm of frequency. To do this only the isotherms showing a maximum of ϵ'' were considered. These isotherms superpose very well in the low frequency side of the relaxation but not so well in the high frequency side probably because of the overlapping of the secondary relaxation that appears at temperatures just below the glass transition [33]. On the Fig. 8 the line corresponding to the KWW equation, i.e., Eq. (1) with

$$\phi(t) = \exp\left(-\left(\frac{t}{\tau_D}\right)^{\beta_D}\right), \tag{19}$$

with $\beta_D = 0.35$ is shown. The agreement between this value and its counterpart in the calorimetric structural relaxation is excellent as has been found in several amorphous polymers [54,56,57]. The dielectric relaxation time can be calculated from the position of the maximum of ϵ'' at each temperature in the frequency axis f_{max} as $\log(2\pi f_{max}\tau_D(T)) = -0.20$ for this value of the KWW exponent [64]. The values of the dielectric relaxation time as a function of temperature were represented in Fig. 6. The temperature dependence of the dielectric relaxation times show the characteristic curvature of the of the main dielectric relaxation in amorphous

polymers, with values lower than the calorimetric ones. These DRS data were fitted to the VFTH equation log $\tau_D = 11.6 - 348.2/(T\text{-}233.7)$ and from this equation the slope *Ea/R* defined again from Eq. (18) was calculated and it is represented by the full line in Fig. 7. The value of $T_0 = 233.7$ K in VFTH equation obtained from dielectric results agrees with the value of $T_2 = 229.5$ obtained by modelling of the DSC results with $B = 500$ J/g.

Dielectric relaxation spectroscopy gives information on the conformational mobility at temperatures above the glass transition, i.e., in structural equilibrium. To compare the dielectric response of the main-chain segments with the calorimetric one at temperatures below T_g, in the glassy state, the thermally stimulated depolarization current, TSDC, dielectric technique is specially suitable because of its low equivalent frequency and high resolution power. In TSDC experiments the polymer sample is polarized by application of a constant electric field at a temperature T_p high enough to ensure that the permanent dipoles of the polymer chains (in the case of the α relaxation those situated along the main-chain) are oriented in the direction of the applied field. The sample is then cooled down to a temperature T_s, low enough, at which the molecular mobility of the groups in which the dipoles reside is frozen. The sample is then short-circuited. No reorientation of the dipoles takes place because of the lack of molecular mobility. The sample is then subjected to a heating ramp at constant rate and intensity of the depolarizarion current, $i(T)$, because of the release of the frozen-in polarization is recorded. All the experimental details are in Ref. [31]. The result of such as global depolarization process in LCP1 [33,65] is shown in Fig. 9. For values of T_p and T_s, well above and below T_g respectively, the peak in $i(T)$, with a maximum close to the calorimetric glass transition temperature, proves that the reorientation of the main-chain dipoles, and thus, the main-chain mobility starts at temperatures below T_g, in the glassy state.

A detailed study of the conformational mobility in a particular temperature interval can be achieved by means of the thermal sampling experiments. In these experiments the sample is polarized at a temperature T_p for a time t_p and the polarizing field is kept while the sample is cooled to a temperature T_d, being the interval $T_p - T_d$, or polarizing window, typically 2°–5°. The sample is short-circuited at T_d and the cooling process continues to T_s. The depolarization curve $i(T)$ measured in the heating scan is representative of the relaxation process of the molecular groups that are mobile in the temperature interval of the polarizing window. From the $i(T)$ curve it is possible to calculate the apparent activation energy of this "elemental" relaxation process (see [33] and the references cited therein). In the case of the α relaxation process, the results of thermal sampling experiments with values of the polarizing temperature immediately below T_g are representative of the conformational mobility of the LCP1 main-chains in the glassy state (secondary relaxation processes appears at lower temperatures in the glassy state). From the experimental data taken from Refs. [33,65] the apparent activation energy was calculated and it is represented as a function of the temperature of the maximum of the depolarization peak in Fig. 7 together with its counterparts in DRS and DSC experiments. Taking into account the differences between the definition and calculation procedure of *Ea* in each technique, the parallelism between dielectric and calorimetric behaviour is quite apparent.

4.3. A picture of the vitrification of the side-chain liquid–crystal polymer

The aforementioned DSC and DRS data show a close relationship between the α dielectric relaxation process and the calorimetric glass transition. Not only both processes take place in the same temperature interval but also the temperature dependence of the relaxation times and the width of the distribution of relaxation times are quite similar. This could be surprising at first sight taking into account that the α dielectric relaxation is detected through the motion of the permanent dipoles contained in the mesogens, thus in the side chains, while the calorimetric glass transition is usually related to the conformational rearrangements of the main-chain segments. Nevertheless a quite consistent picture of what is happening in this relaxation process can be achieved taking into account the co-operative nature of the glass transition phenomenon through the coupling between the motions of the main-chain segments and the mesogens in the glass transition.

In terms of the Adam–Gibbs theory a co-operative rearranging region CRR is defined as a region of the material which contains a number of molecules or polymer segments that can undergo a conformational transition without disturbing the rest of the material, i.e. with no motion of the molecules or polymer segments outside the CRR.

In the case of an amorphous polymer such as poly(vinyl acetate) it has been shown [59] that a co-operative conformational rearrangement involves around five simultaneous or sequential motions in main-chain segments. In other words, when a conformational motion in a main chain segment takes place four other main chain segments are forced to move. The conformational rearrangement takes place in a volume of around 15 nm^3. The case of a side-chain liquid crystal polymer is quite different. If the polymer chains are randomly distributed including random positions of the mesogens, a CRR contains a number of mesogens, main-chain atoms and spacer atoms. In order to have an intuitive image of such a CRR one can just take the O, Si or C atoms as volume units. Thus, a 11% of the volume of the CRR would be occupied by O or Si atoms of the main chain or methyl groups directly bonded to Si, while a 54% would be occupied by mesogens and a 30% by atoms pertaining to the spacer or the end of the side-chain to leave a 5% of free volume.

In this situation, the closest neighbour to a main-chain

segment is probably not another main-chain segment but a mesogen or atom pertaining to the spacer. The coupling between the motions of main-chains and mesogens has to be understood in the sense that a co-operative conformational rearrangement inside a CRR involves the motion of mesogens together to the main-chain and spacer atoms.

From the point of view of the dielectric relaxation the explanation would be similar. At low temperatures only local motions of the mesogens are possible. These local motions produce the secondary β relaxations [11,14,15]. The α relaxation appears when, under the electric field applied, the orientation of the mesogen can push apart the main-chain segments and other mesogens situated in its neighbourhoud in a co-operative motion.

Both techniques DRS and DSC probe the same molecular phenomenon in the glass transition region, involving the coupled motions of main-chain and side-chains. This phenomenon is also probed by dynamic-mechanical relaxation spectroscopy according to the results reported in Ref. [66].

This interpretation is not contradictory with the fact that a δ relaxation occurs at higher temperatures. The permanent dipole residing in the mesogen could be not fully reoriented in a time compatible with the frequency of the dielectric field applied through the co-operative motions that can take place in the glass transition, and another relaxation would take place when the free volume is higher.

By contrast, a glass transition with no participation of the mesogenic groups needs the existence of large enough regions, in the order of magnitude of the correlation length, in which the nearest neighbour of a main-chain segment is another main-chain segment or atoms pertaining to the spacer. This kind of microheterogeneity is not possible even in the case of the liquid–crystal smectic order because the spacer is not long enough to allow the polymer main chains to pack together apart from the mesogens.

It is interesting to refer, in this context, that for relatively short spacers (say, up to eight methyl units), the dynamic correlation between the polymer backbone and the mesogenic groups may depend on the spacer length [67]. This behaviour was found by looking at the degree of cooperativity, in terms of the coupling model proposed by Ngai, in mechanical and dielectric results on side-chain LCPs with different spacer lengths.

5. Concluding remarks

The modelling of the DSC thermograms by means of phenomenological models allows to calculate the relaxation times of the structural relaxation process from the experimental results consisting of a series of $c_p(T)$ curves measured after different thermal histories. Different calculations procedures allow to estimate the same value parameter β of the KWW relaxation function which is 0.35 for this liquid-crystalline polymer, a value that is in close agreement with the one determined for the dielectric relaxation process that appears in the temperature interval immediately above the calorimetric glass transition. It is possible to determine the temperature dependence of the relaxation times both in equilibrium (which can be compared with the relaxation times of the main dielectric or dynamic-mechanical relaxation processes) and in the glassy state. The ratio of the apparent activation enthalpy in the liquid to that of the glassy states x can also be determined in a very consistent way, following different methods from the experimental results. The value of the apparent activation energy in equilibrium, around T_g: $\Delta h^*/R = 85$ kK was determined experimentally from the dependence of the glass transition temperature with the cooling rate and also from the modelling of the experimental thermograms obtained after different thermal histories with very good agreement. The parallelism between the temperature dependence of the dielectric and calorimetric relaxation times in equilibrium and in the glassy state was shown. Thus, it can be concluded that the modelling of the structural relaxation process is a useful tool to determine the characteristic of the conformational rearrangements in amorphous materials. In the liquid crystalline polymer which is the subject of this work DSC and DRS probes the same molecular phenomenon: the co-operative conformational rearrangements involving coupled motions of the main-chain segments and the mesogenic side-chain groups.

Acknowledgement

J.M.M.D. and J.L.G.R. wish to acknowledge the support of CICYT through MAT97-0634-C02-01.

References

[1] Gordon M, editor. Advances in poymer science-liquid-crystalline polymers. Berlin: Springer, 1985.
[2] Cifferi A, editor. Liquid-crystallinity in polymers: principles and fundamental properties. Weinheim, New York, Cambridge: VCH, 1991.
[3] McArdle CB, editor. Side-chain liquid crystalline polymers. London: Blackie, 1988.
[4] Fawcett AH, editor. High value polymers. Special pub. no. 87. Royal Society of Chemistry, Cambridge, 1991.
[5] Finkelmann H, Portugall M, Ringsdorf H. Am Div Polym Chem 1978;19:183.
[6] Finkelmann H, Naegele D, Ringsdorf H. Makromol Chem 1979;180:803.
[7] Plate NA, Shibaev VP. Comb-shaped polymers and liquid crystals. New York: Plenum Press, 1987.
[8] Kresse H, Talroze VR. Makromol Chem Rapid Commun 1981;2:369.
[9] Kresse H, Kostromin S, Shibaev VP. Makromol Chem Rapid Commun 1982;3:509.
[10] Böhme A, Novotna E, Kresse H, Kuschel F, Lindau J. Makrom Chem 1993;194:3341.
[11] Zentel R, Strobl GR, Ringsdorf H. Macromolecules 1985;18:960.
[12] Kremer F, Vallerien SU, Zentel R, Kapitza H. Macromolecules 1989;22:4040.
[13] Vallerien SU, Kremer F, Boeffel C. Liq Cryst 1989;4:9.

[14] Colomer FR, Meseguer Dueñas JM, Gómez Ribelles JL, Barrales-Rienda JM, Bautista de Ojeda JM. Macromolecules 1993;26:155.
[15] Gedde UW, Liu F, Hult A, Sahlen F, Boyd RH. Polymer 1994;35:2056.
[16] Schönhals A, Geβner U, Rübner J. Macromol Chem Phys 1995;196:1671.
[17] Haase W, Pranoto H, Bormuth F. Ber Bunsenges Phys Chem 1985;89:229.
[18] Pranoto H, Bormuth F, Haase W, Kieghle V, Finkelmann H. Makrom Chem 1986;187:2453.
[19] Bormuth F, Haase W. Mol Cryst Liq Cryst 1987;148:1; Bormuth F, Haase W. Mol Cryst Liq Cryst 1987;153:207.
[20] Attard GS, Williams G. Polym Commun 1986;27:2; Attard GS, Williams G. Liq Cryst 1986;1:253; Attard GS, Williams G, Gray GW, Lacey D, Gemmel PA. Polymer 1986;27:185.
[21] Attard GS, Moura Ramos JJ, Williams G. J Polym Sci 1987;25:1099.
[22] Araki K, Attard GS, Kozak A, Williams G, Gray GW, Lacey D, Nestor GJ. J Chem Soc Faraday Trans II 1988;84:1067.
[23] Williams G, Nazemi , Karasz FE, Hill JS, Lacey D, Gray GW. Macromolecules 1991;24:5134.
[24] Nazemi A, Williams G, Attard GS, Karasz FE. Polym Adv Technol 1992;3:157.
[25] Williams G. Polymer 1994;35:1915 and references therein.
[26] Andrews SR, Williams G, Läsker L, Stumpe J. Macromolecules 1995;28:8463.
[27] Seiberle H, Stille W, Strobl G. Macromolecules 1990;23:2008.
[28] Zhong ZZ, Schuele DE, Smith SW, Gordon L. Macromolecules 1993;26:6403.
[29] Zhong ZZ, Gordon WL, Schuele DE, Akins RB, Percec V. Mol Cryst Liq Cryst 1994;238:129.
[30] Zhong ZZ, Schuele DE, Gordon WL. Liq Cryst 1994;17:199.
[31] Kim HJ, Jackson R, Simon GP. Eur Polym J 1994;30:1201.
[32] Alegría A, Echave JM, Davis FJ, Guo W, Mitchell GR. J Non-Cryst Solids 1994;172–174:966.
[33] Mano JF, Correia NT, Moura Ramos JJ, Andrews SR, Williams G. Liq Cryst 1996;20:201.
[34] Attard GS. Mol Phys 1986;58:1087.
[35] Maier VW, Saupe A. Z Naturf A 1959;14:882; Maier VW, Saupe A. Z. Naturf.A 1960;15:287; Maier VW, Meier G. Z Naturf A 1961;16:262.
[36] Nordio PL, Rigatti G, Segre U. Molec Phys 1973;25:129.
[37] Williams G. Chem Rev 1972;72:55.
[38] Davies RO, Jones GO. Adv Phys 1953;2:370.
[39] Scherer GW. J Non-Cryst Solids 1990;123:75.
[40] Hodge IM. J Non-Cryst Solids 1994;169:211.
[41] Hutchinson JM. Prog Polym Sci 1995;20:703.
[42] Narayanaswamy OS. J Am Ceram Soc 1971;54:491.
[43] Moynihan CT, Macedo PB, Montrose CJ, Gupta PK, DeBolt MA, Dill JF, Dom BE, Drake PW, Esteal AJ, Elterman PB, Moeller RP, Sasabe H. Ann NY Acad Sci 1976;279:15.
[44] Scherer GW. J Am Ceram Soc 1984;67:504.
[45] Hodge IM. Macromolecules 1987;20:2897.
[46] Kovacs AJ, Aklonis JJ, Hutchinson JM, Ramos AR. J Polym Sci 1979;17:1097.
[47] Williams G, Watts DC. Trans Faraday Soc 1970;66:80.
[48] Adam G, Gibbs JH. J Chem Phys 1965;43:139.
[49] Gibbs JH, DiMarzio EA. J Chem Phys 1958;28:373.
[50] Prest WM, Roberts FJ, Jr, Hodge IM. Proceedings of the Twelfth NATAS Conference, 1980, p. 119–123.
[51] Tribone JJ, O Reilly JM, Greener J. Macromolecules 1986;19:1732.
[52] Romero Colomer F, Gómez Ribelles JL. Polymer 1989;30:849.
[53] Gómez Ribelles JL, Ribes Greus A, Diaz Calleja R. Polymer 1990;31:223.
[54] Gómez Ribelles JL, Monleón Pradas M. Macromolecules 1995;28:5867.
[55] Gómez Ribelles JL, Monleón Pradas M, Vidaurre Garayo A, Romero Colomer F, Más Estelles J, Meseguer Dueñas JM. Polymer 1997;38:963.
[56] Brunacci A, Cowie JMG, Ferguson R, Gómez Ribelles JL, Vidaurre Garayo A. Macromolecules 1996;29:7976.
[57] Meseguer Dueñas JM, Vidaurre Garayo A, Romero Colomer F, Más Estellés J, Gómez Ribelles JL, Monleón Pradas M. J Polym Sci 1997;35:2201.
[58] Montserrat S, Gómez Ribelles JL, Meseguer Dueñas JM. Polymer 1998;39:3801.
[59] Gómez Ribelles JL, Vidaurre Garayo A, Cowie JMG, Ferguson R, Harris S, McEwen IJ. Polymer 1998;40:183.
[60] Mohynihan CT, Easteal AJ, DeBolt MA, Tcker J. J Amer Ceram Soc 1976;59:12.
[61] O'Reilly JM, Hodge IM. J Non-Cryst Solids 1991;131-133:451.
[62] Simon SL. Macromolecules 1997;30:4056.
[63] Nedler JA, Mead R. Comput J 1965;7:308.
[64] Williams G, Watts DC, Dev SB, North AM. Trans Faraday Soc 1971;67:1323.
[65] Mano JF. PhD Thesis. Universidade Técnica de Lisboa, Instituto Superior Técnico. Lisboa, 1996.
[66] Simon GP, Kozak A, Williams G, Wetton. Materials Forum 1991;15: 71.
[67] Ngai KL, Etienne SS, Zhong ZZ, Schuele DE. Macromolecules 1995;28:6423.